

## Cubic-to-Tetragonal Transformation and Susceptibility in $\text{LaAg}_x\text{In}_{1-x}$ Alloys\*

H. Ihrig, D. T. Vigen, J. Kübler, and S. Methfessel

*Abteilung für Physik, Ruhr-Universität, Bochum, Germany*

(Received 14 May 1973)

The magnetic susceptibility  $\chi(x, T)$  of the pseudobinary intermetallic compound  $\text{LaAg}_x\text{In}_{1-x}$  is given for temperatures  $T$  between 20 and 250 K with  $x$  between 1.0 and 0.15. For  $x$  between 0.9 and 0.6,  $\chi$  is very anomalous, rising strongly as the samples are cooled until a temperature  $T_M(x)$  is reached where a cubic-to-tetragonal crystallographic transformation is found to occur and the susceptibility drops to a much lower value. The transformation is shown to arise from a band Jahn-Teller effect. The behavior of  $\chi(x, T)$  as well as  $T_M(x)$  can be described quantitatively over a broad range of  $x$  assuming that the Fermi energy of LaAg lies closely below a high peak in the density of states which originates from the  $e_g$  states of La. This peak becomes gradually populated as the electron concentration is increased by replacing Ag by In.

### I. INTRODUCTION

The characteristics of valence and conduction electrons are of fundamental importance for the structure of metals and alloys<sup>1,2</sup> and the relationship between electronic properties and crystal structure has assumed a strong theoretical posture within the formalism of pseudopotential theory.<sup>3</sup> Unfortunately, pseudopotential theory relies rather heavily on the wide-band properties of electrons; therefore, it works best for  $s$ - $p$  bonded metals, but poorly for narrow bands.

Recently, work on  $A$ -15 intermetallic compounds<sup>4</sup> (high-temperature superconductors which transform structurally from a cubic to a tetragonal phase in the normal state) shows that the narrow  $d$  bands of the transition elements can be all important in determining the stable crystallographic structure.<sup>5-10</sup> Since effects of a tetragonal deformation on the electronic  $d$  bands are presumably too small to be resolved in band-structure calculations, special models must be developed to describe the experimental observations. One rather successful approach for the  $A$ -15 compounds is the band analog of the Jahn-Teller effect due to Labbé and Friedel.<sup>5-7</sup>

The essential idea is that a lattice deformation partially removes the degeneracy of  $d$  subbands which may lie in the vicinity of the Fermi level, causing a repopulation of the various subbands, and resulting in a lowering of the crystal-free energy. Because the  $A$ -15 compounds possess linear chains of transition-metal ions, the theory of Labbé and Friedel employs a one-dimensional density of states for the  $d$  subbands. Although their model seems to depend heavily on the one dimensionality, Cohen *et al.*<sup>8</sup> and Rehwald *et al.*<sup>9</sup> were able to explain the elastic and magnetic properties of the  $A$ -15 compound  $\text{Nb}_3\text{Sn}$  by simply assuming a pronounced steplike increase in the density of states just below the Fermi edge. An es-

sential result of the Jahn-Teller model of Labbé and Friedel is the strong dependence of the lattice deformation temperature on the population of states in a high-density-of-states region. Unfortunately, a test of the model by a systematic variation of carrier concentration seems to be impossible in the  $A$ -15 compounds for chemical reasons.

Recently,<sup>11</sup> a cubic-to-tetragonal lattice transformation was discovered in the pseudobinary solid solution of the intermetallic compounds LaAg and LaIn. This is a particularly simple system possessing the cubic CsCl structure at room temperature. Although the compounds show no superconductivity above 2 K, this system is of interest in relation to the  $A$ -15 compounds because one observes here a similar crystallographic transition without chainlike atom arrangements, and one can study the dependence of the transition on the electron concentration over a wide concentration range.

In the first part of this paper we present experimental results on the magnetic susceptibility for the series  $\text{LaAg}_x\text{In}_{1-x}$ . From these measurements the temperature  $T_M$  at which the lattice instability occurs is obtained as a function of  $x$ . Over the concentration range  $0.6 \leq x \leq 0.9$  our susceptibility curves are similar to that obtained for the  $A$ -15 compound  $\text{Nb}_3\text{Sn}$ .<sup>9</sup> Furthermore, the theoretical prediction of the concentration dependence of  $T_M(x)$  based on the Labbé-Friedel model for the  $A$ -15 compounds has the general features of that deduced from our measurements. Therefore, in the second part of the paper we attempt a theoretical interpretation of the experimental data adapting the basic ideas of Labbé and Friedel to our three-dimensional bands using an extension of the model employed by Cohen *et al.*<sup>8</sup> and Rehwald *et al.*<sup>9</sup> For pure LaAg, which remains cubic at low temperatures, the Fermi energy is assumed to be located directly below a pronounced rectangular peak in the density of states. [This assumption is

to a certain extent justified by band-structure calculations performed on YCu<sup>12</sup> which show that such a peak may result in the CsCl-type compounds from the narrow, doubly degenerate  $e_g$  ( $\Gamma_{12}$ ) states of the La ions in their cubic environment.] In a tetragonal environment this peak will be distorted, and the situation is described through a deformation potential. Presuming that the Fermi energy increases with In concentration and that the general features of the density-of-states

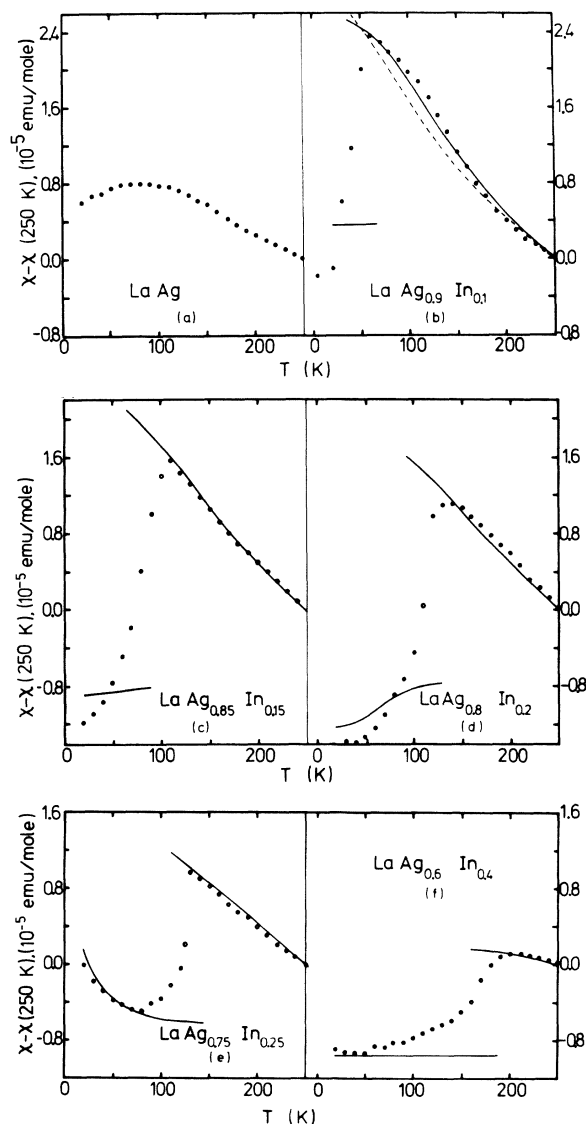


FIG. 1. Magnetic susceptibility of  $\text{LaAg}_x\text{In}_{1-x}$  in the concentration range  $0.6 \leq x \leq 1.0$ . The susceptibility is shown relative to its value at  $T=250$  K, and the solid lines are theoretical fits using parameter values given in Table I. The dashed line in Fig. 1(b) is a best fit with a slightly smaller Fermi energy than that assumed for the solid line, and is used to demonstrate the sensitivity of the fits to this quantity.

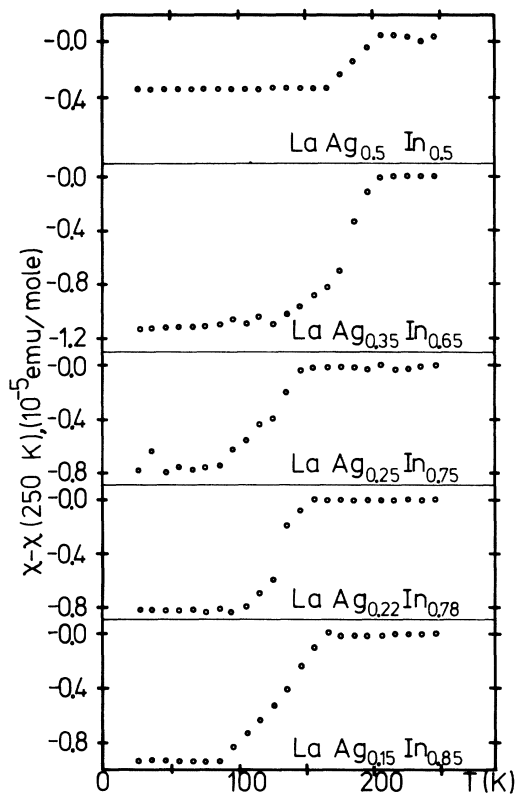


FIG. 2. Magnetic susceptibility of  $\text{LaAg}_x\text{In}_{1-x}$  in the concentration range  $0.15 \leq x \leq 0.5$ . The susceptibility is shown relative to its value at  $T=250$  K.

structure are preserved as the In concentration is increased, we obtain a good description of the concentration dependence of the transformation temperature  $T_M(x)$  and the susceptibility data over a broad range of  $x$ .

## II. EXPERIMENTAL RESULTS

Polycrystalline samples of the pseudobinary intermetallic compound  $\text{LaAg}_x\text{In}_{1-x}$  were prepared from stoichiometric quantities of La, Ag, and In pieces by melting several times in a pure argon arc furnace. The compounds were found to have the cubic CsCl structure at room temperature, and the  $x$  dependence of the residual resistivities indicates that indium replaces silver at random.<sup>11</sup>

The magnetic susceptibility was measured in a Faraday balance for temperatures between 4 and 300 K in cooling runs only. The data were corrected for paramagnetic impurities (a few ppm of Ce in La) by subtracting out the corresponding Curie susceptibility. The corrected susceptibility of  $\text{LaAg}_x\text{In}_{1-x}$ , Figs. 1–3, has its largest inaccuracy at low temperatures ( $T < 40$  K), where the Ce susceptibility becomes large.

The interesting features of the experimental susceptibility are the strong rise in the susceptibility with decreasing temperature (Fig. 1) and the appearance of a "knee" around the crystallographic transformation temperature  $T_M$  (Figs. 1 and 2).<sup>13</sup> Resistivity measurements<sup>11</sup> in  $\text{LaAg}_x\text{In}_{1-x}$  give a hysteresis in cooling and warming runs centered around the same temperature  $T_M$ . The width of this hysteresis could be reduced by annealing, and the temperatures  $T_M$  obtained this way by both resistivity and susceptibility measurements are shown as a function of  $x$  in Fig. 4, the "error bars" giving the approximate widths of the hysteresis.

Detailed x-ray analysis<sup>11</sup> at temperatures below  $T_M$  reveals a tetragonally deformed CsCl structure. The reflections can be indexed by assuming a tetragonal unit cell consisting of eight deformed CsCl cells. Figure 5 compares the lattice constants of the cubic and the tetragonal structure. For a better comparison one-half of the tetragonal lattice constants are plotted.

If the theoretical assumptions made in this paper are correct, one should expect similar phase transformations in a large number of other rare-earth pseudobinary CsCl compounds at isoelectronic compositions. Indeed, a phase transition has been found in  $\text{LaCd}$  at  $T_M = 62$  K, which is only about one-third of the transition temperature found in the isoelectronic composition  $\text{LaAg}_{0.5}\text{In}_{0.5}$ . It is, however, to be expected that the transition depends on the ionic size of the constituents. Accordingly, we find *no* transition in  $\text{YAg}_x\text{In}_{1-x}$  nor in  $\text{GdAg}_x\text{In}_{1-x}$ , but we do find a transition in  $\text{CeAg}_x\text{In}_{1-x}$ , at temperatures comparable with those in  $\text{LaAg}_x\text{In}_{1-x}$ .<sup>14</sup>

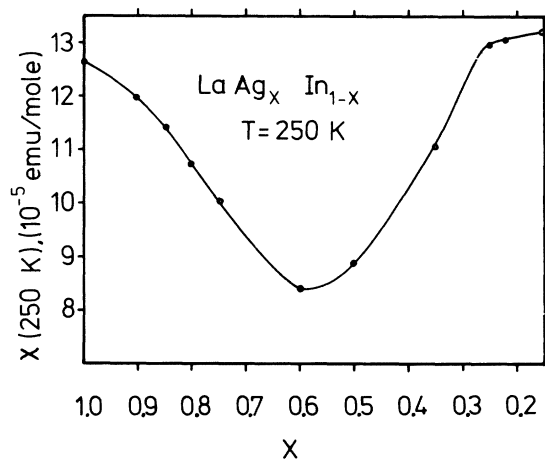


FIG. 3. Absolute magnitude of the magnetic susceptibility of  $\text{LaAg}_x\text{In}_{1-x}$  at  $T = 250$  K as a function of  $x$ .

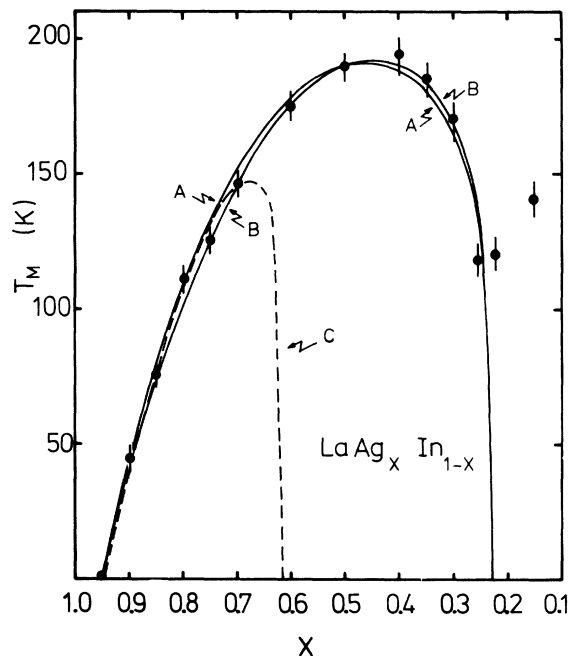


FIG. 4. Crystallographic transformation temperature  $T_M$  as a function of  $x$ . The curves labeled A, B, and C are theoretical fits obtained with different sets of parameter values given in Table III.

### III. THEORY

A good picture of the electronic bands of  $\text{LaAg}$  and  $\text{LaIn}$  would be very helpful in understanding the crystallographic transformation and the anomalous behavior of the susceptibility. Although the bands of these compounds have not been computed, there exists a recent APW calculation of  $\text{YCu}$ <sup>12</sup> which is isostructural to  $\text{LaAg}$  but has the main quantum numbers reduced by 1. Hence similarities in the general character of the bands in both compounds might be expected.

Of particular interest in the  $\text{YCu}$  bands is the position of the Fermi energy, which lies within a rather wide band of mixed  $s$ - $d$  character, directly below a sharp spike in the density of states. This sharp structure originates from a very flat portion of the twofold orbitally degenerate  $e_g$  ( $\Gamma_{12}$ ) band of  $\text{Y}d$  states. We assume that the  $\text{LaAg}$  conduction bands show the same feature.<sup>15</sup>

It is plausible that the  $e_g$  bands formed from the  $d_{3z^2-r^2}$  and  $d_{x^2-y^2}$  states will be very sensitive to tetragonal distortions, for example, on expansion of the lattice along the  $z$  axis, with corresponding compressions along the  $x$  and  $y$  axes. Under such a distortion, the band of the  $d_{x^2-y^2}$  states is broadened owing to greater overlap of the electronic wave functions, whereas the band of the  $d_{3z^2-r^2}$  states is narrowed. Also, the centers of gravity

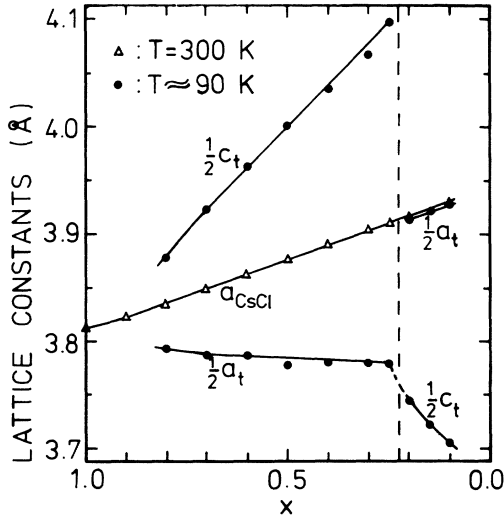


FIG. 5. Lattice constants of  $\text{LaAg}_x\text{In}_{1-x}$  at two temperatures below and above  $T_M$ . The cubic-phase lattice constant is  $a_{\text{CsCl}}$ , the tetragonal-phase lattice constants are  $a_t$  and  $c_t$ .

of the two subbands will, in general, shift since a tetragonal crystal field lifts the orbital degeneracy of the  $e_g$  states. Under circumstances where the Fermi energy lies in the vicinity of these deforming bands, a repopulation of the states occurs which may result in a lower free energy for the crystal. In this case a spontaneous transformation to the tetragonal phase occurs (very much like a Jahn-Teller effect), with corresponding anomalies in the electronic transport and response coefficients.

To render the problem workable, we describe the band structure of cubic  $\text{LaAg}$  in the vicinity of the Fermi energy with the simple density of states model<sup>8</sup> shown in the lower portion of Fig. 6. The density-of-states spike due to the  $e_g$  bands of  $\text{La}$  is approximated by a rectangle of height  $N_0$  and width  $E_0$ , which is superimposed on a broad  $s$ - $d$  conduction band of width  $2E_s$  and relative height  $\alpha N_0$ .

Under a tetragonal distortion, we assume the band widths  $E_1$  and  $E_2$  due to the states  $d_{x^2-y^2}$  and  $d_{3z^2-r^2}$ , respectively, become

$$E_1 = E_0(1 + U_1\epsilon), \quad (1)$$

$$E_2 = E_0(1 - U_2\epsilon), \quad (2)$$

where  $U_1$  and  $U_2$  are (except for a numerical factor) positive deformation potentials and  $\epsilon$  is the strain parameter which is larger than zero if the ratio of the lattice constants  $c/a$  is larger than 1, and  $\epsilon < 0$  if  $c/a < 1$ .

For simplicity we assume

$$U_1 = U_2 = 2U. \quad (3)$$

Then requiring that the total number of states in each subband be the same in the cubic and tetragonal phases, we obtain for the partial density of states

$$N_1(E, \epsilon) = \frac{1}{2}N_0[1 - 2U\epsilon/E_0 + 4(U\epsilon/E_0)^2] \quad (4)$$

if the energy  $E$  is in the interval  $-\epsilon U \leq E \leq (E_0 + \epsilon U)$ , and

$$N_2(E, \epsilon) = \frac{1}{2}N_0[1 + 2U\epsilon/E_0 + 4(U\epsilon/E_0)^2] \quad (5)$$

if  $\epsilon U \leq E \leq (E_0 - \epsilon U)$ , corresponding to the  $d_{x^2-y^2}$  and  $d_{3z^2-r^2}$  states, respectively.

The total density of states

$$N = \alpha N_0 + N_1 + N_2$$

is shown for  $U\epsilon/E_0 = \frac{1}{10}$  in the upper portion of Fig. 6. We ignore any displacement of the center of gravity of the bands due to the tetragonal crystal-field splitting, although this may not be too good an approximation. Also, the background density of states is assumed to be unaffected by the strain.

Having constructed a plausible model for the density of states of  $\text{LaAg}$  near the Fermi edge, we make the rather drastic assumption that this structure remains intact as indium is alloyed. It should be emphasized that this is not an assumption of rigid bands (which would be an extremely poor one since  $\text{Ag}$  and  $\text{In}$  possess valence electrons of different symmetry character); but rather

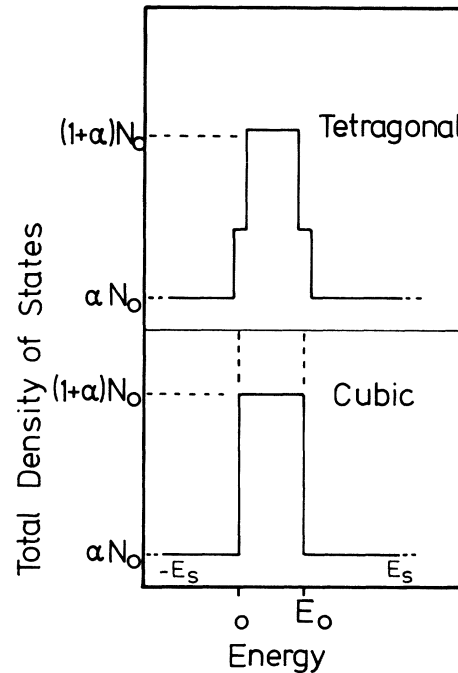


FIG. 6. Model of the total electronic density of states used in the theoretical interpretation of the data.

we assume only that the shape and position of the narrow density-of-states peak produced by the  $e_g$  states of La is unaltered by the replacement of Ag by In. The main effect of this replacement is to cause the Fermi energy, which for pure LaAg is assumed to lie directly below the high density-of-states peak, to shift gradually into the peak. The tendency for the Fermi level to rise is due to the fact that In possesses two more valence electrons than Ag. A surprisingly good explanation of the experimental observations is obtained up to moderately high In concentrations using this simple picture of the electronic structure of the alloy.

We begin by assuming that the free energy  $F$  of the crystal may be written as a sum of two additive parts

$$F = F_0 + F_d. \quad (6)$$

The contribution from the  $d$  electron states of La is contained in  $F_d$ . The contributions of all other electrons are lumped into  $F_0$ .

Treating the electron-electron intra-atomic Coulomb interaction in the Hartree-Fock approximation<sup>16</sup> neglecting interband mixing, we easily obtain the following expression of  $F_d$  in the presence of a weak applied magnetic field  $\vec{H}$ :

$$F_d = \mu Q_d - \frac{kT}{2} \sum_{j,\sigma} \int_{-\infty}^{\infty} N_j(E, \epsilon) \times \ln \left[ 1 + \exp \left( - \frac{E + In_{j,\sigma} + \sigma \mu_B H - \mu}{kT} \right) \right] dE - \sum_j In_{j,n_j}. \quad (7)$$

Here  $\mu$  is the chemical potential,  $Q_d$  the total density of  $d$  electrons in the  $e_g$  subband,  $k$  the Boltzmann's constant,  $T$  the temperature,  $N_j(E, \epsilon)$  the density of states in the  $j$ th subband [ $j=1$  or  $2$ ; cf. Eqs. (4) and (5)],  $I$  the Coulomb interaction constant (normally denoted by  $U$  in Hubbard theories<sup>16</sup>), and  $n_{j,\sigma}$  is the average density of electrons in the  $j$ th subband of spin  $\sigma$  ( $\sigma = \uparrow$  or  $\downarrow$ ), which is given by

$$n_{j,\sigma} = \frac{1}{2} \int_{-\infty}^{\infty} N_j(E, \epsilon) \times \left[ 1 + \exp \left( \frac{E + In_{j,\sigma} + \sigma \mu_B H - \mu}{kT} \right) \right]^{-1} dE, \quad (8)$$

$\mu_B$  being the Bohr magneton.

In Secs. III A and III B, we calculate from the free energy the susceptibility  $\chi$  and the transition temperature  $T_M(x)$ , fitting these quantities independently to experiment with a small set of parameters with physically reasonable values. It will be seen that best fits of  $T_M(x)$  are obtained using values which are not entirely consistent with those used to fit  $\chi$ , although for  $x > 0.6$  a reasonably consistent set can be found which fits both quantities.

### A. Susceptibility Anomalies

We may write the susceptibility  $\chi(x, T)$  as

$$\chi(x, T) = \chi_0(x) + \chi_d(x, T). \quad (9)$$

The major contributions to  $\chi_0(x)$  come from the spin and orbital susceptibility of the electrons in wide bands, the diamagnetic susceptibility of the core electrons, and the Van Vleck paramagnetic susceptibility of the core and band electrons. Since a detailed knowledge of the band structure is required for its computation, any temperature dependence of the band Van Vleck paramagnetism is neglected, although such a term might be significant in La alloys.<sup>17</sup> For the sake of simplicity we assume that the observed  $T$  dependence arises solely from the contribution of the high-density  $e_g$  states  $\chi_d$ . In computing  $\chi_d$ , we assume that the Landau diamagnetism of the  $d$  electrons may be neglected in comparison with the Pauli spin paramagnetism, since the  $d$  electrons have a large effective mass.

We treat the  $d$  electrons in the Hartree-Fock approximation, obtaining an explicit expression for  $\chi_d$  by direct differentiation of Eq. (7),

$$\chi_d = - \left( \frac{\partial^2 F_d}{\partial H^2} \right)_{H=0} = \mu_B^2 \sum_{j=1}^2 N_j^{\text{eff}} / \left( 1 - \frac{1}{4} IN_j^{\text{eff}} \right), \quad (10)$$

where the temperature-dependent effective density of states  $N_j^{\text{eff}}$  is given as

$$N_j^{\text{eff}} = N_j f_j(E_j^l). \quad (11)$$

Here the  $N_j$  are given by Eqs. (4) and (5) and  $f_j(E)$  is

$$f_j(E) = \left[ 1 + \exp \left( \frac{E + \frac{1}{2} In_j - \mu}{kT} \right) \right]^{-1}, \quad (12)$$

where  $E_j^l$  refers to the energy of the lower edge of the  $j$ th subband, and  $n_j$  is the total density of electrons in the  $j$ th subband.

Equations (10)–(12) give the enhanced susceptibility for two subbands in the Hartree-Fock approximation. In obtaining these expressions we have assumed that the number of electrons in the  $d$  band is small. Equation (10) may be written explicitly for the two structural phases in our model as

$$\chi_d^{\text{cubic}} = \mu_B^2 N_0 f(0) / \left[ 1 - \frac{1}{4} IN_0 f(0) \right] \quad (13)$$

and

$$\chi_d^{\text{tetra}} = \frac{\mu_B^2 N_0}{2} \left( \frac{f(U'\epsilon)}{1 - \frac{1}{4} IN_0 f(U'\epsilon)} + \frac{f(-U'\epsilon)}{1 - \frac{1}{4} IN_0 f(-U'\epsilon)} \right). \quad (14)$$

Here  $U'\epsilon$  is a Hartree-Fock renormalized deformation potential defined by

$$U'\epsilon = U\epsilon - \frac{1}{4}I(n_1 - n_2), \quad (15)$$

and is assumed to be small compared to  $E_0$ . In Eq. (15) we see that the second term is strain dependent, making the renormalization approximately zero for small strains ( $n_1 \approx n_2$ ), and a maximum of  $\frac{1}{4}IQ_d$  when the strain is large enough so that the narrowed subband is almost entirely depopulated ( $n_1 \approx Q_d$ ,  $n_2 \approx 0$ ).

The Fermi function appearing in Eqs. (13) and (14) is given by

$$f(E) = (1 + e^{(E - \mu')/kT})^{-1}, \quad (16)$$

where

$$\mu' = \mu - \frac{1}{4}IQ_d.$$

As usual, conservation of the total number of electrons (in this case  $e_g$  plus wide-band  $s$ - $d$  electrons) determines  $\mu'$  and hence  $f(E)$ . In the cubic phase the conservation equation can be manipulated into the form

$$f^{\alpha/(\alpha+1)} = (1 - f)e^{(E'_F/kT)} \quad (17)$$

if  $E'_F > 0$  and

$$(1 - f)^{(\alpha+1)/\alpha} = f e^{-E'_F/kT} \quad (18)$$

if  $E'_F < 0$  and can be solved numerically for arbitrary  $\alpha$ .

The quantity  $E'_F$  is the Hartree-Fock renormalized Fermi energy [defined as the cubic phase limit  $\mu'(T \rightarrow 0) \equiv E'_F$ ]

$$E'_F = E_F / (1 + \frac{1}{4}IN_0), \quad (19)$$

and  $f \equiv f(0)$  is the Fermi function evaluated at the lower  $e_g$  band edge. In the tetragonal phase the equation for particle conservation is difficult to solve for arbitrary  $\alpha$ . However, if  $\alpha$  can be assumed small (which, in fact, we shall do), the conservation equation takes the form

$$e^{\mu'/kT} = [\cosh^2(U'\epsilon/kT) + e^{(2E'_F/kT)} - 1]^{1/2} - \cosh(U'\epsilon/kT). \quad (20)$$

Figures 1(a)–1(f) show the variation of  $\chi(x, T)$  with respect to its value at  $T = 250$  K for a number of indium concentrations. When 10% of Ag has been replaced by In [Fig. 1(b)], the susceptibility changes radically, showing a rapid increase with decreasing temperature, with a large drop appearing at  $T_M$ . We attribute this anomalous behavior to the entering of the Fermi energy into the narrow  $e_g$  band of La, which is assumed to be empty for pure LaAg.

The experimental susceptibility of  $\text{LaAg}_x\text{In}_{1-x}$  for a silver concentration between 0.6 and 0.9 can easily be fitted in the cubic phase with Eqs. (13)

TABLE I. Parameter values used in the theoretical fits of  $\chi(x, T)$  of  $\text{LaAg}_x\text{In}_{1-x}$ . The quantities  $E'_F$  and  $U'\epsilon$  are the Fermi energy and the deformation energy, respectively.

$x$	$E'_F$ (K)	$U'\epsilon$ (K)
0.9	250	420
0.85	300	420
0.8	350	420
0.75	440	420
$\leq 0.6$	$> 1000$	$> 3000$

and (17), the observed temperature dependence requiring the Fermi energy  $E'_F$  to be given by the numbers listed in Table I.

In the tetragonal phase the susceptibility is then fitted with Eqs. (14) and (20) using the deformation energy  $U'\epsilon$  as given in Table I. Compatible with the parameters given in Table I is a concentration-independent set of values for  $N_0$ ,  $I$ , and  $\alpha$ :  $N_0 = 1.55$  states/eV atom,  $I = 0.548$  eV, and  $\alpha = 0.25$ . The theoretical fits are included as solid lines in Figs. 1(b)–1(f), which demonstrate good agreement between our simple Hartree-Fock theory and experiment.

Table I indicates that our model breaks down for  $x \leq 0.6$ , at least in a detailed description of the susceptibility, signifying that a radical departure from our density of states picture occurs at this point. For this reason the data shown in Fig. 2 have not been fitted.

Figure 3 shows the absolute magnitude of the susceptibility  $\chi$  at 250 K versus silver concentration  $x$ . Over the concentration range  $0.6 \leq x \leq 0.9$ , where our model seems to have validity, one can deduce the contribution  $\chi_0(x)$  to the susceptibility defined by Eq. (9); it is given in Table II.

### B. Crystallographic Transformation Temperature

In order to determine the tetragonal instability, we consider the crystal to be in zero applied magnetic field. Then Eq. (7) becomes

$$F_d = \mu Q_d - kT \sum_{j=1}^2 \int_{-\infty}^{\infty} N_j(E, \epsilon) \times \ln \left[ 1 + \exp \left( - \frac{E + \frac{1}{2}In_j - \mu}{kT} \right) \right] dE - \frac{1}{4} \sum_{j=1}^2 In_j^2. \quad (21)$$

Here  $n_j$  is the electron density in the  $j$ th subband, and  $N_j(E, \epsilon)$  is given by Eqs. (4) and (5). The elastic modulus ( $C_{11} - C_{12}$ ) is obtained by

$$C_{11} - C_{12} = \left( \frac{\partial^2 F}{\partial \epsilon^2} \right)_{\epsilon=0} \quad (22)$$

TABLE II. Values of the temperature-independent susceptibility  $\chi_0(x)$  of  $\text{LaAg}_x\text{In}_{1-x}$  deduced from the experimental susceptibility at  $T=250$  K.

$x$	0.9	0.85	0.80	0.75
$\chi_0(x)$ ( $10^{-5}$ emu/mole)	8.12	7.12	6.09	4.91

in the cubic state. Since the stable value of  $\epsilon$  is that which minimizes  $F$ , the condition  $(C_{11} - C_{12}) \leq 0$  indicates an instability of the cubic phase. By means of Eqs. (6), (21), and (22) one obtains for the elastic modulus

$$C_{11} - C_{12} = (a_{11} - a_{12}) - U^2 N_0 A(T). \quad (23)$$

Here  $A(T)$  is given by

$$A(T) = f - \frac{IN_0(E'_F/E_0 - \frac{1}{2}f)}{1 + \frac{1}{4}IN_0 f} + \frac{4kT}{E_0} \ln(1-f) + 4 \left( \frac{kT}{E_0} \right)^2 [2L_2(f) + \ln^2(1-f)], \quad (24)$$

where  $E'_F$  is the Hartree-Fock renormalized Fermi energy given by Eq. (19),  $L_2$  is the dilogarithm function defined by<sup>18</sup>

$$L_2(x) = - \int_0^x \frac{\ln(1-y)}{y} dy, \quad (25)$$

and  $f=f(0)$  is the Fermi function, Eq. (16), evaluated at the lower  $e_g$  band edge.

The quantity  $(a_{11} - a_{12})$  in Eq. (23) is defined by

$$a_{11} - a_{12} = \left( \frac{\partial^2 F_0}{\partial \epsilon^2} \right)_{\epsilon=0}. \quad (26)$$

It is the contribution to the elastic modulus from all sources contained in  $F_0$  and is in general positive and weakly temperature dependent. We ignore this temperature dependence. The second term on the right-hand side of Eq. (23) gives the part of  $(C_{11} - C_{12})$  due to the  $e_g$  states. It is a negative contribution which "softens" the elastic modulus, and so is totally responsible for the tetragonal instability. The temperature  $T_M$  where the instability occurs is obtained from the condition

$$(a_{11} - a_{12})/U^2 N_0 = A(T_M). \quad (27)$$

In deriving Eqs. (23) and (24) we have assumed that only a rather small number of electrons is in the  $e_g$  band at  $T=0$ . One arrives at a completely symmetric result for small hole concentrations (almost filled  $e_g$  states). As in the theory of Labbé and Friedel,<sup>5-7</sup> no tetragonal instability is possible for large electron (or hole) concentrations. This is in contrast to the theory of Rehwalde *et al.*<sup>9</sup> It is contained in our theory and can be most easily seen by observing that the quantity  $A(T)$  is a monotonically decreasing function of

temperature, attaining its maximum value in the limit  $T \rightarrow 0$ :

$$A(T=0) = \frac{(2E'_F/E_0 - 1)^2}{1 + \frac{1}{4}IN_0}. \quad (28)$$

From Eqs. (27) and (28) one first sees that a tetragonal instability is possible only if

$$U^2 N_0 > (a_{11} - a_{12}) (1 + \frac{1}{4}IN_0). \quad (29)$$

Hence the instability is initiated when the product of the deformation potential with the density of states is large. Secondly, if Eq. (29) is satisfied, the maximum Fermi energy  $E'_F$  for which the instability can occur is given by

$$E'_F = \frac{1}{2}E_0 \{1 - [\gamma(1 + \frac{1}{4}IN_0)]^{1/2}\}, \quad (30)$$

where

$$\gamma = (a_{11} - a_{12})/U^2 N_0. \quad (31)$$

The cubic phase is always stable for  $E'_F \leq 0$  and for  $E'_F \leq E'_F \leq \frac{1}{2}E_0$ . (Corresponding results obtain for holes in a more than half-filled band.)

At first we attempt to fit  $T_M(x)$  over the widest concentration range possible, irrespective of the parameter values assumed in the susceptibility fits of Sec. IV A. One may calculate  $T_M$  from Eqs. (24), (27), and (17), once a relation between the Fermi energy  $E'_F$  and the In concentration is assumed. We use the simple form

$$E'_F = (0.95 - x)b, \quad (32)$$

where  $b$  is a constant. This form satisfies the requirement that  $E'_F = 0$  for  $x = 0.95$ . [From experiment  $T_M = 0$  at this concentration, and from Eqs. (27), (28), and (29) we see that this requires  $E'_F = 0$ .]

There is a simple relation between  $E'_F$  defined by Eq. (30) and that Fermi energy  $E'_F$  where the maximum  $T_M$  occurs, namely,

$$E'_F/E'_F = \frac{5}{2} [1/(1 + \sqrt{\gamma})]. \quad (33)$$

Experimentally, the maximum  $T_M$  of about 192 K (cf. Fig. 4) occurs for  $x_m = 0.45$ ; and since the critical concentration corresponding to  $E'_F$  can reasonably be chosen as  $x_c = 0.24$ , one obtains from Eqs. (32) and (33)  $\gamma = 0.578$ . After a choice is made for the  $s$ - $d$  conduction-band density-of-states parameter  $\alpha$ , the remaining parameters  $E_0$ ,  $b$ , and  $IN_0$  can be deduced from the experimental slope of  $T_M$  vs  $x$  at  $x = 0.95$  and the maximum  $T_M$  of  $T_M = 192$  K.

The two solid curves of Fig. 4, labeled A and B, are fits of the data using the correspondingly labeled sets of parameter values listed in Table III. These curves are representative of those given by the other unlabeled sets of values in Table III. From Table III one sees immediately that the only sensitive parameter is the Fermi en-

TABLE III. Parameter values used in the theoretical fits of the crystallographic transformation temperature  $T_M$  of  $\text{LaAg}_x\text{In}_{1-x}$ . First column is the experimental slope of  $T_M$  vs  $x$  at  $x=0.95$ . The quantities  $\alpha$ ,  $IN_0$ ,  $E_0$ , and  $b$  are, respectively, the contribution to the density of states due to the  $s$ - $d$  conduction electrons, the intra-atomic Coulomb interaction times density of  $e_g$  states, bandwidth of  $e_g$  states, and Fermi energy divided by  $(0.95-x)$ .

$-\left(\frac{dT_M}{dx}\right)_{x=0.95}$ (K)	$\alpha$	$IN_0$	$E_0$ (K)	$b$ (K)	Fit shown in Fig. 4
860	0.0	0.45	5953.2	829.2	B
	0.1	0.7	6897.7	852.8	...
	0.2	0.85	7574.8	866.9	...
	0.3	1.0	8465.7	892.3	...
1000	0.0	no fit	...	...	...
	0.25	0.2	5160.9	802.0	A
	0.75	0.75	7142.4	861.1	...
	1.5	1.0	8473.4	893.1	...
860	0.25	0.85	79580.0	2550.0	C

ergy, the quantity  $b$  varying less than 100 K for all fits with the quality represented by curves A and B of Fig. 4.

It should be emphasized here that fits A and B of Fig. 4 are made using parameter values which are not consistent with those used to fit  $\chi$ . The model is successful in fitting  $T_M(x)$  over a much wider  $x$  range than  $\chi$ , and in order to see if this result is only fortuitous, it is worthwhile to attempt a fit of  $T_M(x)$  using parameter values that are as consistent as possible with the susceptibility fits. This is shown as the dashed curve C in Fig. 4, using  $\gamma=0.79$  and the values labeled C in Table III. The parameters used for curve C are completely consistent with those of the  $\chi$  fits except for  $E'_F(x)$ , for which no completely consistent values can be found. Comparison of  $E'_F(x)$ , needed to fit  $\chi$  and  $T_M$ , is made in Fig. 7. Best fits of  $T_M(x)$  (curves A and B of Fig. 4) are made with the solid straight line; whereas the fit most consistent with the  $\chi$  fits (curve C of Fig. 4) is made with the dashed straight line. The solid curved line in Fig. 7 is that used to fit  $\chi(x, T)$ . The  $\chi$  fits are found to be very sensitive to the value of  $E'_F$ . An example of this sensitivity is shown in Fig. (1b), where the dashed curve represents a fit using  $E'_F=200$  K and the solid curve represents a fit using  $E'_F=250$  K. It should be emphasized that each of these fits was made independently, using the best possible values of the other parameters.

#### IV. DISCUSSION

We have shown that the behavior of the measured susceptibility  $\chi(x, T)$  of  $\text{LaAg}_x\text{In}_{1-x}$  can be explained for  $0.6 \leq x \leq 0.9$  using a simple density-of-states model and giving a small set of param-

eters physically reasonable values, under the assumption that the observed structural instability arises from a bandlike Jahn-Teller effect and that the increase in In concentration causes a general increase in the Fermi energy  $E'_F$  into a fixed density-of-states peak. The description is not con-

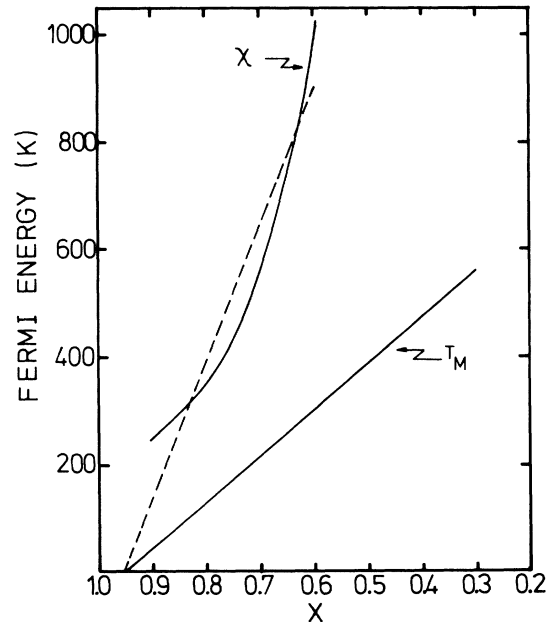


FIG. 7. Fermi energy  $E'_F$  vs  $x$  in  $\text{LaAg}_x\text{In}_{1-x}$ . The solid straight line is used to fit the transition temperature  $T_M(x)$  in the range  $0.25 \leq x \leq 1.0$ . The dashed straight line is used to fit  $T_M(x)$  in the range  $0.6 \leq x \leq 1.0$ , whereas the solid curved line is used to fit the susceptibility  $\chi(x, T)$  in the range  $0.6 \leq x \leq 1.0$ .



sistent, however, since the value of the Fermi energy needed to fit the temperature dependence of  $\chi$  is always larger than that needed to predict correctly the crystalline-phase transition temperature  $T_M(x)$ . (A similar discrepancy was found by Rehwald *et al.*<sup>9</sup> in  $\text{Nb}_3\text{Sn}$ .) In fact, a good description of  $T_M(x)$  is obtained over the much larger concentration region  $0.25 \leq x \leq 1.0$  within the same model, but using values of  $E_F'$  completely inconsistent with the fits of  $\chi$ . Using the most consistent values of  $E_F'(x)$  possible, a good description of  $T_M(x)$  is obtained for  $0.6 < x \leq 1.0$ , and the theoretical fits of  $\chi$  and  $T_M(x)$  break down at approximately the same value of  $x$ . It should be noted that this most consistent fit of  $T_M(x)$  uses a value  $\sim 7$  eV for the  $d$  band width as compared to a value  $\sim 0.7$  eV used for the wider  $x$ -range fits of  $T_M(x)$ . The larger value of  $E_0$  might be in more reasonable agreement with  $d$  bandwidths in transition elements, but one expects narrower bands in alloys since the transition metal ions are more widely separated in this case. The width of the density-of-states peak due to the La- $e_g$  electrons should be even smaller than this.

The breakdown of our theoretical description at the larger In concentrations is probably due to substantial departures from our density-of-states model. The supposition that radical changes in the electronic structure do occur in the In-rich solid solutions is supported by the fact that compounds with  $x \leq 0.1$  cannot be prepared in a one-to-one stoichiometry. The value  $N_0 = 1.55$  states/eV

atom deduced from the fits to  $\chi$  is reasonable for a narrow  $d$  band, being much larger than that of an ordinary wide  $s$  band. The same value  $IN_0 = 0.85$  may be used in good fits of both  $T_M$  and  $\chi$ . Since  $IN_0$  enters the enhanced susceptibility formulas, Eqs. (13) and (14), with a factor  $\leq \frac{1}{4}$ , this value is felt to be not unreasonable.

In order to fit the difference in  $\chi$  at  $T_M$  for the two phases, we must use  $U'\epsilon = 420$  K for all  $x$  values in the range  $0.6 < x \leq 0.9$ . In this concentration range both  $\epsilon$  and the cubic-phase lattice parameter increase (Fig. 5). This implies that the deformation potential  $U'$  decreases since for larger ionic separations the overlap of the  $d$ -band orbitals changes less with applied strain. The fact that a constant  $\gamma = (a_{11} - a_{12})/U^2N_0$  was needed in fitting  $T_M(x)$  could imply that  $(a_{11} - a_{12})$  becomes softer as In is added.

Direct calculation of  $U'\epsilon$  from minimizing the free energy gives a value which, in contrast to the values given in Table I, increases somewhat with increasing In concentrations, but is of the same order as  $U'\epsilon$  deduced from the  $\chi$  fits. It should be pointed out that our model cannot predict whether a structure with a  $c/a$  ratio smaller or larger than 1 is stable since the free energy is symmetric,  $F(\epsilon) = F(-\epsilon)$ . Whereas our theory clearly describes a second-order phase transition, it is not clear from the experimental material at hand whether the crystal transformation observed in  $\text{LaAg}_x\text{In}_{1-x}$  (and similarly in  $\text{LaCd}$ ,  $\text{CeAg}_x\text{In}_{1-x}$ ) is of first or second order.

\*Sponsored in part by the Deutsche Forschungsgemeinschaft.

<sup>1</sup>N. F. Mott and H. Jones, *The Theory and Properties of Metals and Alloys* (Oxford U. P., London, 1936).

<sup>2</sup>W. Hume-Rothery, *Phase Stability in Metals and Alloys*, edited by P. S. Rudman (McGraw-Hill, New York, 1966), p. 3.

<sup>3</sup>V. Heine and D. Weaire, in *Solid State Physics*, edited by H. Ehrenreich, F. Seitz, and D. Turnbull (Academic, New York, 1970), Vol. 24, p. 249.

<sup>4</sup>B. T. Matthias, T. H. Geballe, and V. B. Compton, *Rev. Mod. Phys.* **35**, 1 (1963).

<sup>5</sup>J. Labbé and J. Friedel, *J. Phys. (Paris)* **27**, 153 (1966); *J. Phys. (Paris)* **27**, 303 (1966); *J. Phys. (Paris)* **27**, 708 (1966).

<sup>6</sup>J. Labbé, *Phys. Rev.* **158**, 647 (1967); *Phys. Rev.* **158**, 655 (1967).

<sup>7</sup>J. Labbé, thesis (University of Paris, 1968) (unpublished).

<sup>8</sup>R. W. Cohen, G. D. Cody, and J. J. Halloran, *Phys. Rev. Lett.* **19**, 840 (1967).

<sup>9</sup>W. Rehwald, M. Rayl, R. W. Cohen, and G. D. Cody, *Phys. Rev. B* **6**, 363 (1972).

<sup>10</sup>W. Dieterich and W. Klose, *Z. Phys.* **246**, 323 (1971).

<sup>11</sup>H. Balster, H. Ihrig, and S. Methfessel, *Verh. Dtsch. Phys. Ges.* **8**, 527 (1973).

<sup>12</sup>M. Belakhovsky, J. Pierre, and D. K. Ray, *Phys. Rev. B* **6**, 939 (1972).

<sup>13</sup>A similar behavior of the susceptibility has been observed in other CsCl compounds, as for instance V-Ru alloys [see C.W. Chu, E. Bucher, A.S. Cooper, and J.P. Maita, *Phys. Rev. B* **4**, 320 (1971)].

<sup>14</sup>H. Ihrig, thesis (Ruhr University, Bochum, 1973) (unpublished).

<sup>15</sup>Another argument in favor of similarities in the band structure of YCu and LaAg is a crystallographic transformation of YCu at around 100 K which we found by measuring its resistivity. However, the low-temperature phase of YCu seems to be more complicated than that of  $\text{LaAg}_x\text{In}_{1-x}$ .

<sup>16</sup>D. Wagner, *Introduction to the Theory of Magnetism* (Pergamon, New York, 1972), p. 225.

<sup>17</sup>A. M. Clogston, V. Jaccarino, and Y. Yafet, *Phys. Rev.* **135**, A650 (1964).

<sup>18</sup>I. A. Stegun, *Handbook of Mathematical Functions*, edited by M. Abramowitz and I. A. Stegun (Dover, New York, 1965), p. 1004.